

On the sociology and hierarchy of voids: a study of seven CAVITY nearby galaxy voids and their dynamical CosmicFlows-3 environment

H.M. Courtois^{*1}, R. van de Weygaert², M. Aubert¹, D. Pomarède³, D. Guinet¹, J. Domínguez-Gómez⁴, S. Duarte-Puertas^{5,6}, E. Florido^{4,7}, L. Galbany^{8,9}, R. García-Benito⁵, J.M. van der Hulst², K. Kreckel¹⁰, R.E. Miura^{11,4}, I. Pérez^{4,7}, S. Planelles^{12,13}, V. Quilis¹², J. Román^{2,14,15}, and M. Sánchez-Portal¹⁶

¹ Université Claude Bernard Lyon 1, IUF, IP2I Lyon, 69622 Villeurbanne, France

² Kapteyn Astronomical Institute, University of Groningen, PO Box 800, 9700 AV Groningen, The Netherlands

³ IRFU, CEA Université Paris-Saclay, 91191 Gif-sur-Yvette, France

⁴ Departamento de Física Teórica y del Cosmos, Campus de Fuente Nueva, Edificio Mecenaz, Universidad de Granada, E-18071, Granada, Spain

⁵ Instituto de Astrofísica de Andalucía - CSIC Glorieta de la Astronomía E-18008, Granada, Spain

⁶ Département de Physique, de Génie Physique et d'Optique, Université Laval, and Centre de Recherche en Astrophysique du Québec (CRAQ), Québec, QC, G1V 0A6, Canada

⁷ Instituto Carlos I de Física Teórica y Computacional, Facultad de Ciencias, E-18071 Granada, Spain

⁸ Institute of Space Sciences (ICE, CSIC), Campus UAB, Carrer de Can Magrans, s/n, E-08193 Barcelona, Spain

⁹ Institut d'Estudis Espacials de Catalunya (IEEC), E-08034 Barcelona, Spain

¹⁰ Astronomisches Rechen-Institut, Zentrum für Astronomie der Universität Heidelberg, Mönchhofstrasse 12-14, D-69120 Heidelberg, Germany

¹¹ National Astronomical Observatory of Japan, National Institutes of Natural Sciences, 2-21-1 Osawa, Mitaka, Tokyo 181-8588, Japan

¹² Departamento de Astronomía y Astrofísica, Universidad de Valencia, c/ Dr. Moliner n 50, 46100 - Burjassot (Valencia), Spain

¹³ Observatori Astronòmic, Universitat de València, E-46980 Paterna (València), Spain

¹⁴ Departamento de Astrofísica, Universidad de La Laguna, E-38206, La Laguna, Tenerife, Spain

¹⁵ Instituto de Astrofísica de Canarias, c/ Vía Láctea s/n, E-38205, La Laguna, Tenerife, Spain

¹⁶ Institut de Radioastronomie Millimétrique (IRAM), Av. Divina Pastora 7, Local 20, 18012 Granada, Spain

Received A&A Nov 29, 2022 - AA/2022/45578 / Accepted date

ABSTRACT

Context. The present study addresses a key question for our understanding of the relation between void galaxies and their environment: the relationship between luminous and dark matter in and around voids.

Aims. To explore how empty of matter local Universe voids are, we study the full (dark+luminous) matter content of seven nearby cosmic voids that are fully contained within the CosmicFlows-3 volume.

Methods. The cosmic voids matter density profiles are independently obtained using two different methods. They are built on one hand from the galaxy redshift space 2 points-correlation function and, on the other hand, using peculiar velocity gradients from the CosmicFlows-3 dataset.

Results. The results are noticeable since when using the redshift survey, all voids show a radial positive gradient of galaxies, while based on the dynamical analysis, only three of these voids display a clear underdensity of matter in their center.

Conclusions. It is the first time such a detailed observational analysis of voids is conducted, showing that void emptiness should be derived from dynamical information. Yet, from this limited study, the Hercules void is the best candidate for a local Universe pure "pristine volume" expanding in 3 directions with no dark matter located in that void.

Key words. Cosmology: large-scale structure of Universe

1. Introduction

Galaxies are not evenly distributed in space. Instead, they probe the underlying inhomogeneous dark matter distribution. On Megaparsec scales, matter and galaxies have organized themselves in a weblike network, the Cosmic Web (Bond et al. 1996; Cautun et al. 2014). Prominent elongated filaments define a pervasive structure, assembling most of the matter and galaxies in

the Universe and representing the intergalactic transport channels along which mass is migrating towards the dense, compact clusters and the nodes of the web. An equally outstanding aspect of the weblike cosmic mass distribution is that of the nearl empty void regions (e.g. Kirshner et al. 1981; de Lapparent et al. 1986; Huchra et al. 2012). They are enormous regions with sizes in the range of $20 - 50 h^{-1}$ Mpc that are significantly less populated of galaxies than filaments and clusters. Voids usually are roundish in shape and occupying the major share of space

* helene.courtois@univ-lyon1.fr

(see e.g. van de Weygaert & Platen 2011; van de Weygaert 2016, for reviews). They may assume around 75 – 80% of space (eg. Cautun et al. 2014).

The dominant voids in the cosmic matter distribution are manifestations of the cosmic structure formation process transitioning to the non-linear stage of evolution (Blumenthal et al. 1992; Sheth & van de Weygaert 2004). Their effective repulsive influence over the surroundings has even been recognized in the CosmicFlows - peculiar velocity surveys of the Local Universe (Courtois et al. 2012; Tully et al. 2014). The expansion of the voids makes them into organizing elements of the large scale matter distribution, playing an essential role in arranging matter concentrations into an all-pervasive cosmic network (e.g. Icke 1984; Sheth & van de Weygaert 2004; Aragon-Calvo & Szalay 2013).

Many recent studies followed up on the realization that voids not only represent a key constituent of the cosmic mass distribution, but that they are also one of the cleanest probes of global cosmology (Goldberg & Vogeley 2004; Park & Lee 2007; Lavaux & Wandelt 2012; Bos et al. 2012; Pisani et al. 2015; Hamaus et al. 2016; Cai et al. 2015; Perico et al. 2019). Particularly interesting is the realization that their structure, morphology and dynamics reflect the nature of dark energy, dark matter and that of the possibly non-Gaussian nature of the primordial perturbation field (see Pisani et al. 2019, for a review). The effects of dark energy and possible modifications of General Relativity manifest themselves more prominently in their low density interior.

The interior of voids also offer a unique testing ground for studying environmental influences on galaxy formation and evolution (Peebles 2001; Rojas et al. 2004, 2005; Kreckel et al. 2011, 2012). The low density void interior is a largely pristine cosmic environment that still retains the memory of initial condition, unaffected by virialization or other nonlinear effects. Equivalent to a lower Ω_m universe (Goldberg & Vogeley 2004), galaxies in voids are expected to evolve more slowly and have a calmer merging history (also see Lackner et al. 2012). As a result, they appear to have significantly different properties than average field galaxies.

In general, void galaxies are small, faint and blue galaxies (Kreckel et al. 2011), that appear to reside in a more youthful state of star formation than galaxies in denser environments (Beygu et al. 2016; Domínguez-Gómez et al. 2022). Nonetheless, while these trends appear to be quite general, controversy persists in the literature as to whether or not galaxies in voids genuinely differ in their internal properties from similar objects in denser regions. For example, while Rojas et al. (2005) found evidence for a significantly higher specific star formation rate for void galaxies, other studies (Beygu et al. 2016, eg) did not find evidence for void galaxies to have star formation rates in excess of what might be expected for the small mass they have. It is a well established fact that there are systematic differences in the mass of halos and galaxies residing in different cosmic web environments: with respect to the generic filament environment of galaxies, the void galaxy population mass function is shifted to lower masses and lower number densities (Cautun et al. 2014; Ganeshiah Veena et al. 2019; Hellwing et al. 2021, see eg.). The key question is whether the observed systematic differences between galaxies in voids, filaments, walls and clusters are only due to the differences in their mass, with other noticeable differences solely a direct consequence of this, or whether there are environment specific factors at play (see e.g. Borzyszkowski et al. 2017; Hellwing et al. 2021). The recent study by Goh et al. (2019) argued for mass being the sole determining factor. On

the other hand, specifically in the case of void galaxies (Peebles 2001) in his seminal study on the *Void Phenomenon* pointed out the unexpected low abundance of low mass and dwarf galaxies in voids. This appears to be difficult to reconcile with mere mass scaling within standard Λ CDM cosmology and may be the strongest indication of specific void environmental processes. Indeed, there are many additional environmental factors and processes that one might expect to contribute to the outcome of the galaxy formation process. For example, a prominent environmental influence is that of the different external tidal forces exerted on a forming halo and galaxy (see eg. van de Weygaert & Babul 1994; Hahn et al. 2007; Yan et al. 2013; Borzyszkowski et al. 2017; Paranjape et al. 2018).

With the purpose of investigating systematic differences between void galaxies and galaxies in more dense environments, the Void Galaxy Survey (VGS) (Kreckel et al. 2011, 2012; Beygu et al. 2016, 2017) has been a multi-wavelength program for studying ~ 60 void galaxies. Each galaxy was selected from the deepest interior regions of identified voids in the SDSS redshift survey on the basis of a geometric-topological watershed technique (Platen et al. 2007), with no a priori selection of intrinsic properties of the void galaxies. The project studied in detail the gas content, star formation history and stellar content, as well as kinematics and dynamics of void galaxies and their companions. One of the most tantalizing findings of the VGS is the possible evidence for cold gas accretion in some of the most interesting objects, amongst which are a polar ring galaxy and a filamentary configuration of void galaxies.

The CAVITY¹ survey (Pérez & al. 2023), the Calar Alto Void Integral-field Treasury survey, is the sequel to the VGS and extends the scope of the observational study of the void galaxies. The CAVITY project concentrates on the determination of the influence of the cosmic environment on galaxy formation and the mass assembly history of void galaxies, and in particular on the drivers for galaxy transformation in voids. Of key importance for the interpretation of the void galaxy measurements, is an insight into the dynamical state of the voids in which they are located and, in particular, also to understand the local relation between both the dark matter and luminous matter context of the voids involved.

The present study addresses a key question for our understanding of the relation between void galaxies and their environment: the relationship between luminous and dark matter in and around voids. To this end, we seek to relate the galaxy distribution in and around a sample of nearby voids with a dynamical study of these voids. The sample consists of seven voids, for which our dynamical study is based on the peculiar velocity measurements and kinematic analysis by the CosmicFlows-3 survey (CF3) (Tully et al. 2016). We use this information to analyse the emptiness of these seven nearby (low redshift) CAVITY voids, and to assess the corresponding relationship to the void galaxy environment.

2. Data: CAVITY & CosmicFlows-3

The seven voids analyzed here are taken from the CAVITY void sample on the basis of them to be located in the CosmicFlows-3 reconstructed volume of the Local Universe.

The CAVITY project targets void member galaxies spread across fifteen singular voids. Seven of these voids are fully included in the CosmicFlows-3 reconstructed volume of Local

¹ <https://CAVITY.caha.es/>

Universe. To identify these voids in this article we will use an internal number label that was given by the CAVITY collaboration. The seven studied voids are named: 355, 439, 474, 487, 727, 738, 941.

2.1. CAVITY

Calar Alto Observatory (CAHA) has selected the CAVITY (Calar Alto Void Integral-field Treasury survey) project as one of the three Legacy projects that will define the Calar Alto Observatory science and technology horizon for the coming years. The CAVITY project main goals are to determine the influence of the environment in the mass assembly of void galaxies, to establish how galaxy formation depends on the larger-scale environment and to identify the main driver of galaxy transformation in voids.

To carry out such detailed study the CAVITY galaxies sample was selected by using the Catalogue of Cosmic Voids based on SDSS DR7 data (Pan et al. 2012). The selected redshift range is between 0.005 and 0.05 to obtain photometric and spectroscopic data reaching high angular resolution and faint galaxies in order to have a representative sample of galaxies within voids. To reach a precise characterisation of the voids, these voids should be fully included in the survey and should contain at least 20 galaxies spread at various void-centric distances. Voids located near the edges of the SDSS footprint were eliminated since their centers and geometries could not be properly assessed. After a careful statistical characterisation of the remaining voids, a sub-sample of voids were selected spanning the largest ranges of effective radii, number of galaxies, and volume number densities of galaxies. This defines a mother sample of around 3,000 galaxies. A sub-sample of the order of 200-300 galaxies are being observed with PMAS instrument (Roth et al. 2005) on the 3.5m telescope of Calar Alto observatory.

2.2. CosmicFlows-3

In order to assess the dynamics of the voids in the CAVITY sample, we use the matter distribution implied by the peculiar galaxy velocities in the CosmicFlows-3 (CF3) catalogue. The third release of the CosmicFlows catalogue compiles about 18,000 measurements of galaxy distances and provides the corresponding cosmography on a 3-dimensional grid in supergalactic coordinates that is used in this article. The recently released fourth version of the CosmicFlows catalog (CF4) delivers about 56,000 galaxies and about 1,000 Type Ia supernovae distance measurements (Tully et al. 2022).

The combined measurements of galaxy luminosity distances and recessional velocities in the CF3 catalogue allows us to map the full matter overdensity field in the local Universe, out to $z < 0.05$. The observational data are combined within an iterative forward modelling analysis (Graziani et al. 2019). This analysis entails a comprehensive incorporation of local over- and underdensities and their associated peculiar (or gravitational) velocity fields.

Assuming that the mass fluctuations $\delta_m(\mathbf{x}, t)$ reside in the linear regime, the full - dark + luminous - matter at position and time (\mathbf{x}, t) is obtained on the basis of the reconstructed full 3D matter peculiar velocity field \mathbf{v}_m by:

$$\nabla \cdot \mathbf{v}_m = -aHf(\Omega_m)\delta_m(\mathbf{x}, t), \quad (1)$$

in which a is the scale factor of the universe, H is the Hubble expansion rate, Ω_m the cosmological mass density parameter and $f(\Omega_m)$ the (linear) structure growth rate (Peebles 1980). The

growth rate $f(\Omega_m)$ depends on the cosmological parameter Ω_m used for the computation. The CF3 density field $\delta_m(\mathbf{x})$ is computed on a 256^3 grid of size $500 \text{ h}^{-1} \text{ Mpc}$. This yields a resolution of about $2 \text{ h}^{-1} \text{ Mpc}$ per voxel (a voxel is the cubic volume in a 3D density grid of side size the resolution of the grid).

3. Void Analysis

Since we intend to compare the matter content of voids inferred from the galaxy redshift distribution to that computed from the peculiar velocity dynamics, we need void identification procedures that allow us to trace voids in the two corresponding situations. The first void detection procedure seeks to trace voids in the discrete spatial distribution of galaxies.

3.1. Void detection and identification in the SDSS galaxy redshift survey

From the galaxy distribution in the SDSS galaxy redshift survey, the CAVITY voids have been identified with the VoidFinder procedure (El-Ad & Piran 1997; Hoyle & Vogeley 2004). The algorithm first classifies survey galaxies into either field or wall galaxies. The wall galaxies are used to define the survey density grid. Starting from empty grid cells, empty spheres are grown and merged into individual voids. This yields a map of voids present in the galaxy distribution. The void centers used in our study are the ones defined by Pan et al. (2012).

3.2. Void characterization and void parameters

Prominent void properties are their size and density profiles.

3.2.1. Void Density Profiles

The prime aspect of our analysis is the comparison and relation between the radial galaxy number density profile $\delta_g(r)$ and the corresponding radial mass density profile $\delta_{m,v}^{CF3}(r)$ of the same void. We seek to establish how far galaxies in and around the voids in our sample trace the underlying mass distribution inferred from the velocity field analysis in the CF3 catalogue.

We have computed the galaxy number density profile $\delta_g(r)$ in voids using redshift survey positions of galaxies (with equation 2). It is estimated by counting the number of SDSS galaxies in various shells of radii r_i/R_v around the center of each void. The profile computation involves 40 radial bins of width $\Delta r = 0.125 R_v$, ranging over the interval $r_i/R_v = 0.0$ to 5.0 . The number counts of galaxies in the radial bins around the void centers are normalized by the number counts of a random galaxy sample that follows the same angular coverage and radial selection function as the galaxy sample, as expressed formally in equation (2), in which the random sample consists of 10 times more objects than the observed galaxy sample.

The resulting radial density profile estimate $\delta_g(r)$ is equal to the radial correlation function $\xi(r)$ around a single void center:

$$\delta_g(r) := \xi(r) = \frac{n_R}{n_D} \frac{D_{vg}(r)}{R_{vg}(r)} - 1. \quad (2)$$

In this expression, we follow the Davis-Peebles estimator of the correlation function (Davis & Peebles 1983). The number of galaxies around the void centers at radius r is given by $D_{vg}(r)$, while the number of galaxies around these void centers, in the

random galaxy sample, is given by $R_{vg}(r)$. The ratio between the total number of data sample galaxies n_D and that in the random sample n_R , n_R/n_D , takes care of the required normalization. Hence, in practice the estimate of $\xi(r)$ is the galaxy number density contrast.

The radial mass density profiles $\delta_{m,v}^{CF3}(r/R_v)$ of each void are determined from the mass density field δ_m reconstruction from the CF3 survey. The mass density field is represented on a 256^3 grid of $2h^{-1}\text{Mpc}$ voxels. The radially averaged mass density profile $\delta_{m,v}^{CF3}(r_i/R_v)$ around voids measures the mean full matter - dark + luminous - density from the void center $r = 0$ to its outskirts $r/R_v > 1$.

To include also the environment of each individual void, the mass and galaxy number density profiles are computed from $r/R_v = 0, \dots, 5$. The profile measures the average matter density in radial shells of width Δr , including the voxels i with a radial distance in the range: $r - \Delta r/2 < r_i < r + \Delta r/2$. It is determined from the grid-based density field $\delta_{m,i}^{CF3}$ as follows:

$$\delta_{m,v}^{CF3}(r/R_v) = \frac{1}{N_{\text{voxel}}} \sum_i \delta_{m,i}^{CF3}. \quad (3)$$

Hence, the void matter density profile computed from the CF3 density grid is basically the average density in radial bins of size $\Delta r = 5/40 = 0.125 R_v$, where N_{voxel} is the number of voxels found at separation r/R_v and δ_i^{CF3} is the value of the CF3 density field in the voxel i found at separation r_i/R_v .

The CF3 grid resolution is $2 h^{-1}\text{Mpc}$, while the CAVITY voids, identified using a galaxy number density field, span an interval of mean effective radii between $15 h^{-1}\text{Mpc} < R_v < 25 h^{-1}\text{Mpc}$.

4. Voids and their large scale environment

In order to be able to interpret our results on the relation between the distribution of galaxies and the total mass in and around voids, centered around the comparison between the radial galaxy and mass density profiles, a visual inspection provides the most direct impression of the large scale environment and setting of the void sample.

Figure 1 is an interactive plot that the reader can use to better grasp the location of the seven voids in comparison with the matter density contrast distribution as computed using the CosmicFlows-3 catalog. Figure 2 is showing the supergalactic SGY-SGZ orientation with a thickness of $-2000 < SGX < 2000$ km/s. This plane helps to see how voids 355 and 738 belong to the same underdense region and may well be accounted as a single "Hercules void". Two voids are located near the back-side infall of Coma supercluster: 487 and 727. Their central overdensity as computed from CF3 is directly linked to this large scale structure.

4.1. Hercules supercluster and Void 355

Figure 3 is showing the region around the Hercules supercluster. Around this large-scale mass concentration our selection has three voids. These are the voids 355 and 738 on the nearer side, the 142 on the far side of the supercluster. Of importance for our purpose is the location of these three voids: while all near the Hercules supercluster, they all are solidly located in the underdense interior of the surrounding mass distribution. It will be an exciting goal of the CAVITY peculiar velocity project to be able

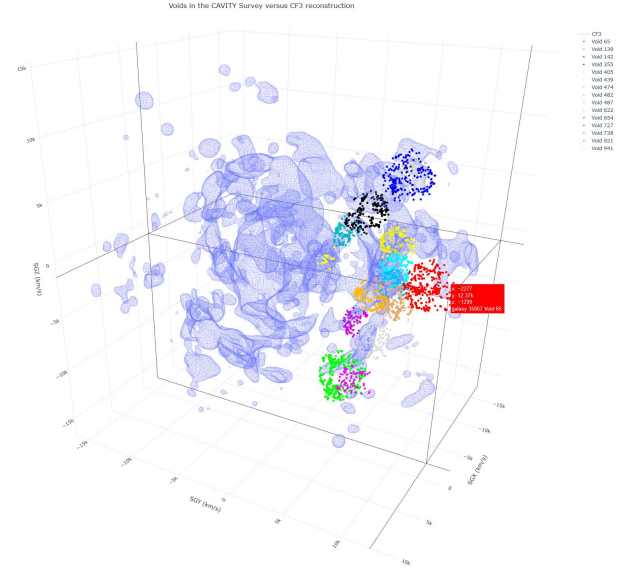


Fig. 1. Interactive 3D visualization of the distribution of nearby voids [Start Interaction]. The positions of the CAVITY survey target galaxies are given using markers colored against their void membership as indicated in the column displayed on the right-hand side. Hover on the galaxy markers to display the galaxy positions, identifiers and void memberships. The wireframe polygon is a high-density ($\delta_m = 1.3$) iso-surface of the reconstructed CosmicFlows-3 overdensity field. Use mouse action to rotate, pan, or zoom in or out. Single-click or double-click on the elements listed on the right-hand side column to hide them or single them out from the scene.

to fully dynamically determine the total mass of the Hercules supercluster.

Figure 4 zooms in on the cosmic V-web (Pomarède et al. 2017) reconstruction, computed using the shear tensor of the peculiar velocity field, in and around Void 355. The color code of the target galaxies are: black, blue, yellow, red if they live in a V-web environment classified as empty, sheet, filament, node, respectively. Iso-surfaces in light grey to dark grey correspond to full matter contrast levels of $\delta_m = -0.3, -0.7, -1.1$, respectively. We can clearly see the galaxies in black (V-Web type: "void") in the center of the void, the blue ones ("sheet") on the periphery, and some yellow ("filament") on the side of Hercules/Great Wall, and there are no galaxy classified in red ("knot"). The CF3 V-web gives a very coherent dynamical pattern of this void 355 for which both galaxy and matter density profiles are in perfect agreement (see fig. 5, and section 5). Also fig. 4 clearly reveals the evacuation by means of the pattern of velocity vectors (black). These depict the local flow, with respect to the center of the underdensity. The interactive version of the figure is made available at [V-web environment of Void 355].

4.2. Coma supercluster and void surroundings

The Coma-Leo complex at the bottom righthand of the mass density map in figure 2 is surrounded by several CAVITY voids. At least three of these, void 482, void 487 and void 727 are lying in or touching the overdense outskirts of the complex. We should not be surprised to find that the galaxy density and the mass density inferred from the CF3 peculiar velocity field may substantially differ. Below we argue that this may be a direct manifestation of the impact of the void environment on the dynamics and evolution of voids.

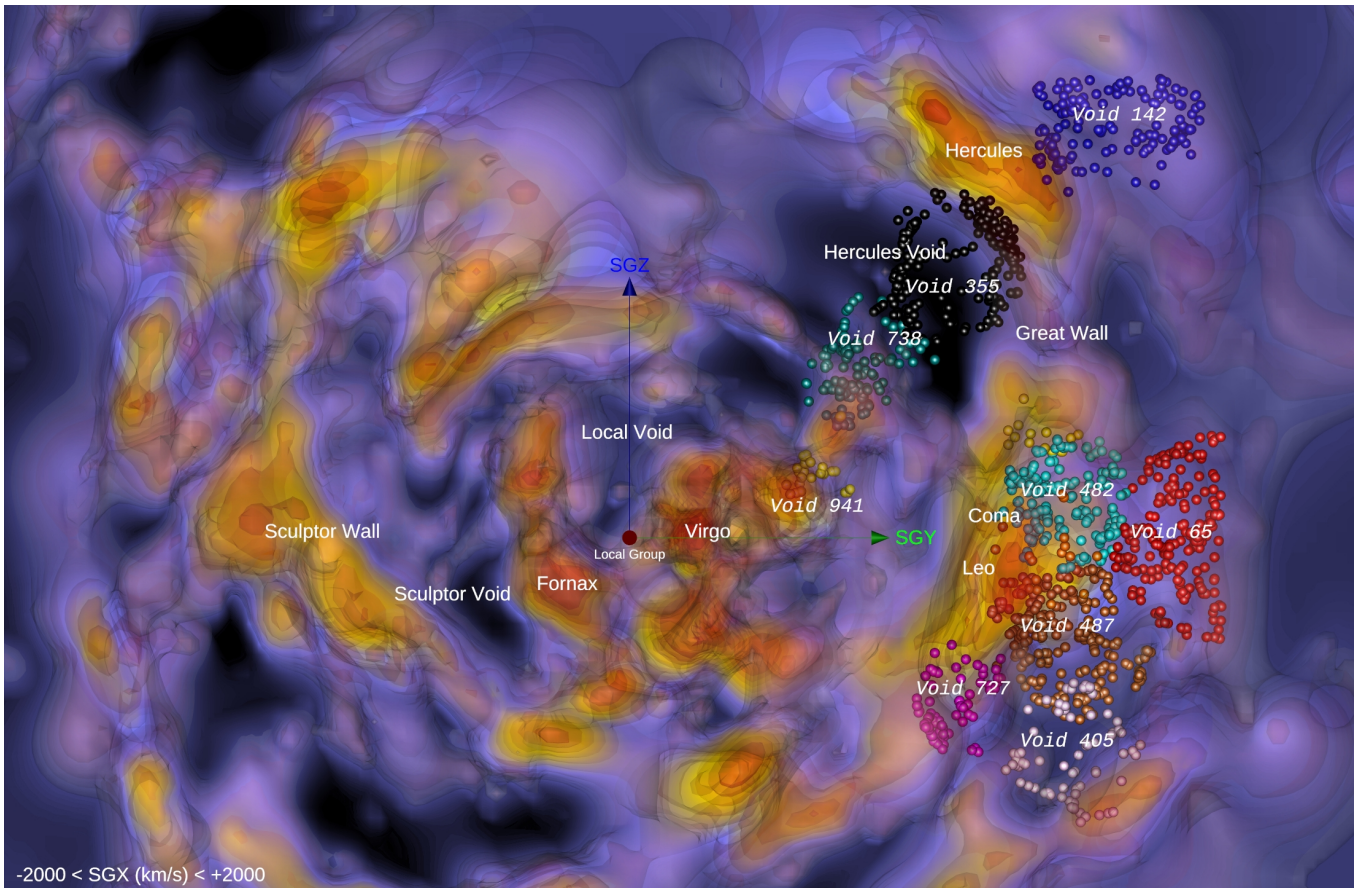


Fig. 2. Map of sample void against reconstructed CosmicFlows-3 density field. Map of galaxy and mass distribution within a slice $-2000 < SGX < 2000$ km/s. Galaxy markers are given distinct colors as a function of their void membership. Scale and orientation are given by the 5000 km/s long green (SGY) and blue (SGZ) arrows emanating from our position, associated with the cardinal axes of the Supergalactic Coordinate System.

4.3. Void Sociology and Hierarchical Void Evolution

The visual appraisal of the void configurations in our study reveal them to provide an interesting and representative mix of voids in different large scale environments. Some are more isolated or remote with respect to overdense mass concentrations - e.g. void 405 and void 738 - while others reside in or near the outskirts of nearby mass concentrations. Voids 355 and 142 are close to the Hercules supercluster, and void 482, void 487 and void 727 are in the outskirts of the Coma region, some almost embedded inside the supercluster. This makes the sample an interesting one for probing the effects of nearby mass concentrations on the dynamics of voids.

Although often the structure and evolution of voids is discussed in terms of singular void configurations (see appendix A), recognizing they are not isolated objects is of key importance for a proper understanding of voids. Given the rather mild level of their density deficit, i.e. $|\delta| < 1$, external mass concentrations remain a major influence in the force inventory of voids (see Sheth & van de Weygaert 2004; van de Weygaert 2016). In fact, when we consider the population of underdensities in the mass distribution, we find that the canonical deep underdense near-spherical void regions that expand in each direction represent a smaller fraction of the void population. Most underdensities may expand along one or two dimensions, but contract along the other directions (Sheth & van de Weygaert 2004; Lavaux & Wandelt 2010). These voids tend to remain smaller, and may even col-

lapse due to the surrounding overdensities. The process goes by the name *void-in-cloud* (Sheth & van de Weygaert 2004).

4.3.1. Hierarchical Void Evolution

On the basis of their hierarchical embedding, we may recognize two principal processes of void evolution (Sheth & van de Weygaert 2004). *Void-in-void* refers to the process in which expanding voids merge into even larger voids, resembling the fate of bubbles in a soap bath (see eg. Dubinski et al. 1993). For voids in or near high density regions that dominate their dynamical evolution, the *void-in-cloud* process refers to the disappearance of voids due to the gravitational contraction and collapse induced by the environment.

The physical context is such that there is a hierarchy of voids, with the velocity field dominated by large expanding voids, in whose interior are found smaller - often elongated - voids, in particular near the edges of large expanding voids (see fig. 11 in van de Weygaert (2016)). They may contract along 1 or 2 dimensions, or even fully collapse. Also important is the fact that many of these voids are not spherical at all, but get substantially deformed by dominant tidal influences of surrounding mass concentrations. It may even involve fully collapsing voids entirely embedded in overdense structures.

The hierarchical void evolution leads to a situation in which it may not be straightforward to relate velocity flow and density in and around voids. As much of the (filtered) flow field includes

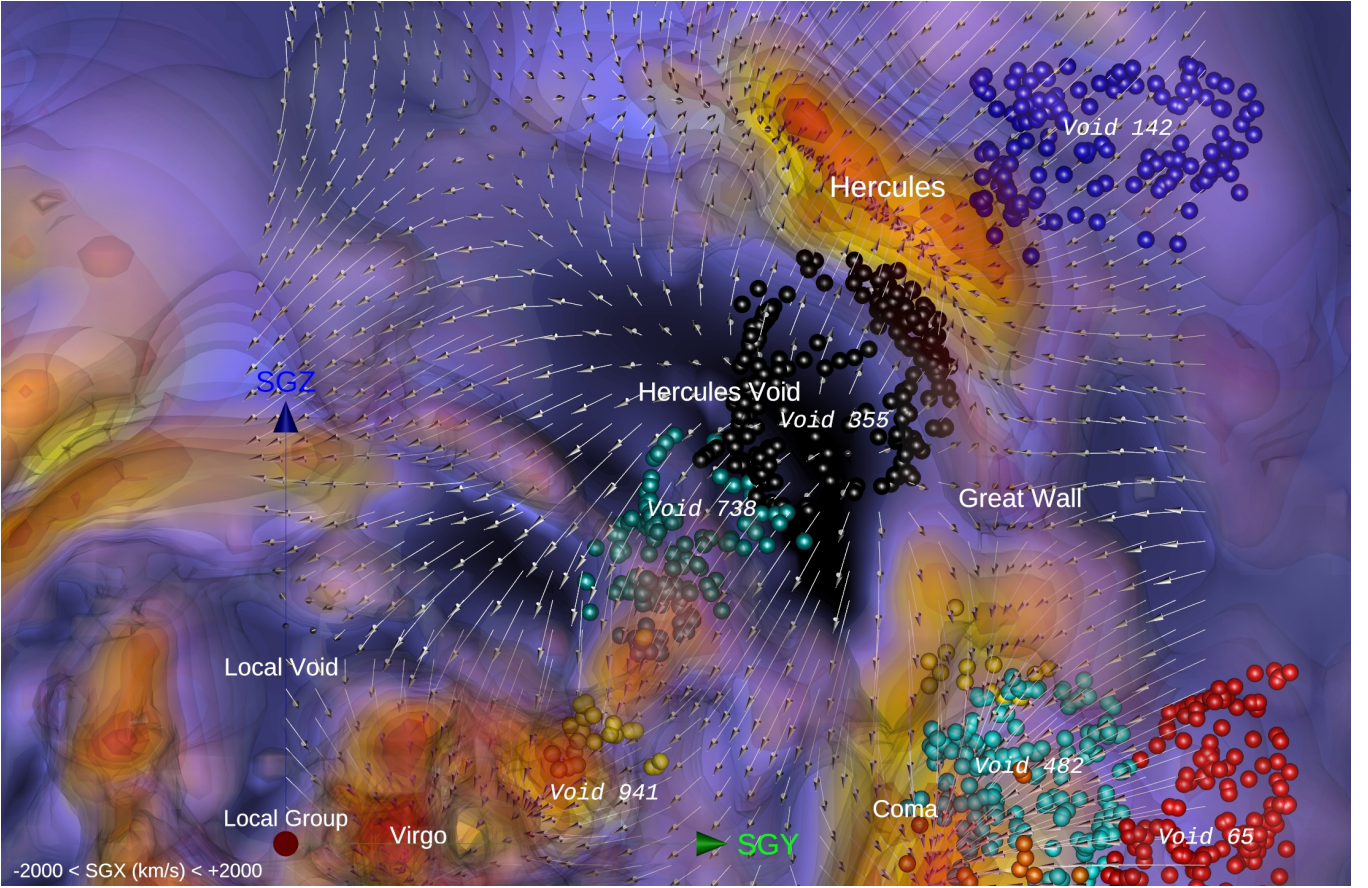


Fig. 3. Voids around the Hercules Void, zoom-in. The positions of galaxies are plotted against the reconstructed CosmicFlows-3 density contrast and velocity field, within a slice $-2000 < SGX < 2000$ km/s. Galaxy markers are given distinct colors as a function of their void membership. Scale and orientation are given by the 5000 km/s long green (SGY) and blue (SGZ) arrows emanating from our position, associated with the cardinal axes of the Supergalactic Coordinate System. The map shows that the galaxies within Void 355 and Void 738 are subject to the evacuation of matter from the Hercules Void, as mapped by the divergent flow at this location.

the dynamical influence of the nearby high density regions. A detailed study and analysis on the the corresponding properties of the hierarchically embedding of void flows, particular in terms of the velocity divergence is Aragon-Calvo & Szalay (2013) (also see Aragon-Calvo et al. 2010).

4.4. Void Environment and Dynamical Impact

Following the observation of the diverse void environments in our sample, and the implications for their dynamical evolution and fate, the quantitative and statistical analysis of the environmental imprint is addressed in the next section, which will show that the visual inspection of the position of voids compared to the well known large scale structures in the local Universe is indeed confirmed quantitatively. The identification of voids in galaxy redshift surveys appears to lead to including voids that appear to partake in the *void-in-cloud* process. Early indications for this had been found in the SDSS survey by the redshift space correlation function analysis by Paz et al. (2013). In other words, our analysis indicates that this is the state of some of the CAVITY voids.

5. Emptiness of voids: results

In this section we compare the δ_g values from galaxy redshift counts to the CF3 reconstruction δ_m contrast field on the basis

of the galaxy and mass density profiles of the seven voids included in our sample. Figure 5 shows the galaxy counts around the seven voids (lefthand panels), together with the mass and galaxy number density profiles (righthand panels).

The lefthand panels of fig. 5 show the number of galaxies in the galaxy samples - SDSS, SDSS void galaxies only and CosmicFlows third and fourth editions - as a function of radial distance (in normalized units) r/R_v . For six voids we see the expected pattern of a steeply increasing number of galaxies as a function of radius, around a near-empty void interior. Only void 941, near the outskirts of the Virgo cluster (see fig. 2), displays a slightly different behaviour. It reveals the presence of many galaxies within half its effective radius R_v .

The galaxy number density profiles (purple dashed lines) and mass density profiles (solid blue lines) do reveal a different story. The profiles in all seven righthand panels do agree on their tendency towards the global mean density value $\delta_m=0$ at $r/R_v > 3$ (the average of the density field over all dimensions in the full CF3 grid gives a value of a mean $\delta_m = 0.005$). This implies that all void configurations consist of a central void surrounded by overdense structures between $1 < r/R_v < 3$. Most importantly is that in at least half of the sample voids there is a strong difference between the computed galaxy number density profile and the mass density profile inferred from the peculiar velocity field.

While the galaxy number density profiles for nearly all sample voids display the well-known “bucket shape” inner profile, the CF3 implied mass profiles do show a different behaviour. For

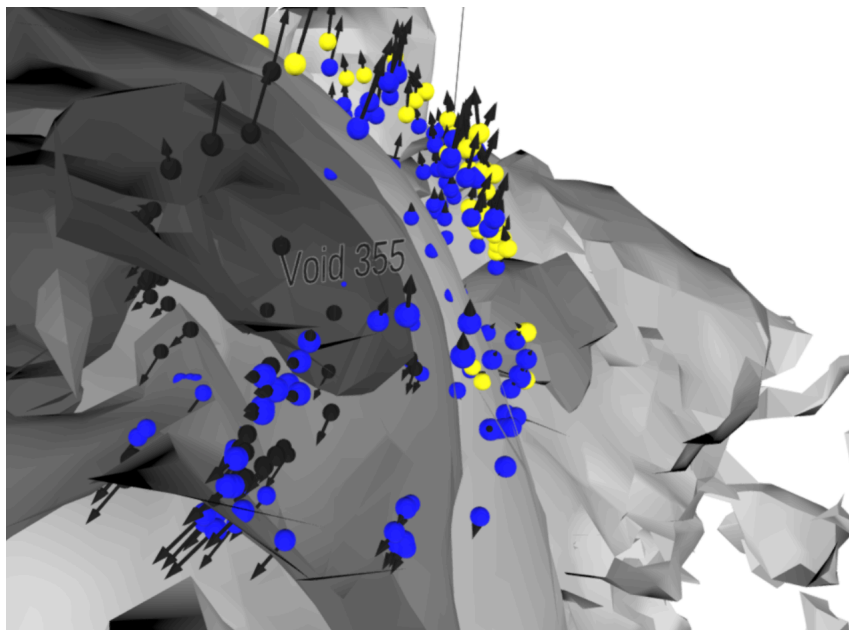


Fig. 4. This figure focuses on the V-web environment as computed using the shear tensor of the CF3 peculiar velocity field for Void 355. The color code of the target galaxies are: black, blue, yellow, red if they live in a V-web environment classified as empty, sheet, filament, node, respectively. Iso-surfaces in light grey to dark grey correspond to full matter contrast levels of $\delta_m = -0.3, -0.7, -1.1$ respectively. One can clearly see the evacuation of the particular speed vectors in black using the local flow (we subtract the speed from the center of the vacuum). The interactive version of the figure is available here: [V-web environment of Void 355].

half of our small sample of seven voids there is strong disagreement in the void emptiness when computed from galaxy counts (empty) and from peculiar velocity dynamics (overdensity near the center). Only in the case of void 355 we find perfect agreement between galaxy and mass density profile. This may relate to the fact that Void 355 is a relatively large and well-defined void of which a significant part is located near the center of the Hercules void mass underdensity. On the other hand, in the case of three, or even four voids, we find implied mass overdensities near the center. In summary, the blue solid lines in fig. 5 show that the CF3 reconstructed matter profiles (computed using equation 3) do not systematically display underdense regions near the voids centers. As we discussed in section 4, some of these voids have centers located in overdense regions in CF3.

Important for the analysis and interpretation of these results is to take into account the differences between the probes used for tracing the CF3 and Cavity probes. The detected voids in different galaxy samples are sensitively dependent on the number density and nature of the galaxy population in those samples (Peebles 2001; Gottlöber et al. 2003; Tinker et al. 2006, see). It is self-evident that voids in more diluted galaxy samples on average will be larger, as these samples lack the spatial resolution to resolve the smaller voids. A more profound influence is the fact that the spatial clustering of galaxies is also sensitively dependent on the galaxies in the sample. Brighter and heavier galaxies are more strongly clustered, and hence will create larger “cavities” in their spatial distribution. A recent study did find that the void population in different galaxy populations is in fact dependent on higher order clustering properties of the galaxy population, in excess of its two-point clustering properties. The found

proof for a strongly systematic dependence of the void population on the topological characteristics of the spatial galaxy distribution (Bermejo et al. 2022). In other words, voids detected in different galaxy populations are strongly affected by a *topological bias*.

Evidence that this subtle galaxy bias effects do affect the void population and inferred void density profiles was already seen in the analysis of voids in the SDSS galaxy survey by Ricciardelli et al. (2013). They found that differences in void probes leads to systematic differences between void density profiles based on galaxy counts and voids extracted from the density distribution in simulations. This may certainly be a factor of relevance in the comparison between the Cavity and CF3 voids in the present study. However, while such biases will undoubtedly play a role, we do not expect them to be able to explain our results as these would even need unrealistic levels of antibias (Braun et al. 1988).

6. Conclusions & Discussion

In the presented analysis we compare the galaxy distribution in and around a small sample of 7 voids from the CAVITY void galaxy survey with the dynamically inferred mass distribution in and around voids. The latter is based on the mass reconstruction from the velocity flow field measured by the Cosmicflows-3 (CF3) survey (Tully et al. 2016). The comparison between the mass and galaxy distribution around these voids, in conjunction with the map of the large-scale mass distribution and features in and around these voids in the Local Universe, enables us to assess the impact of environment on the dynamics and hierarchical evolution of the void population. It demonstrates the reality

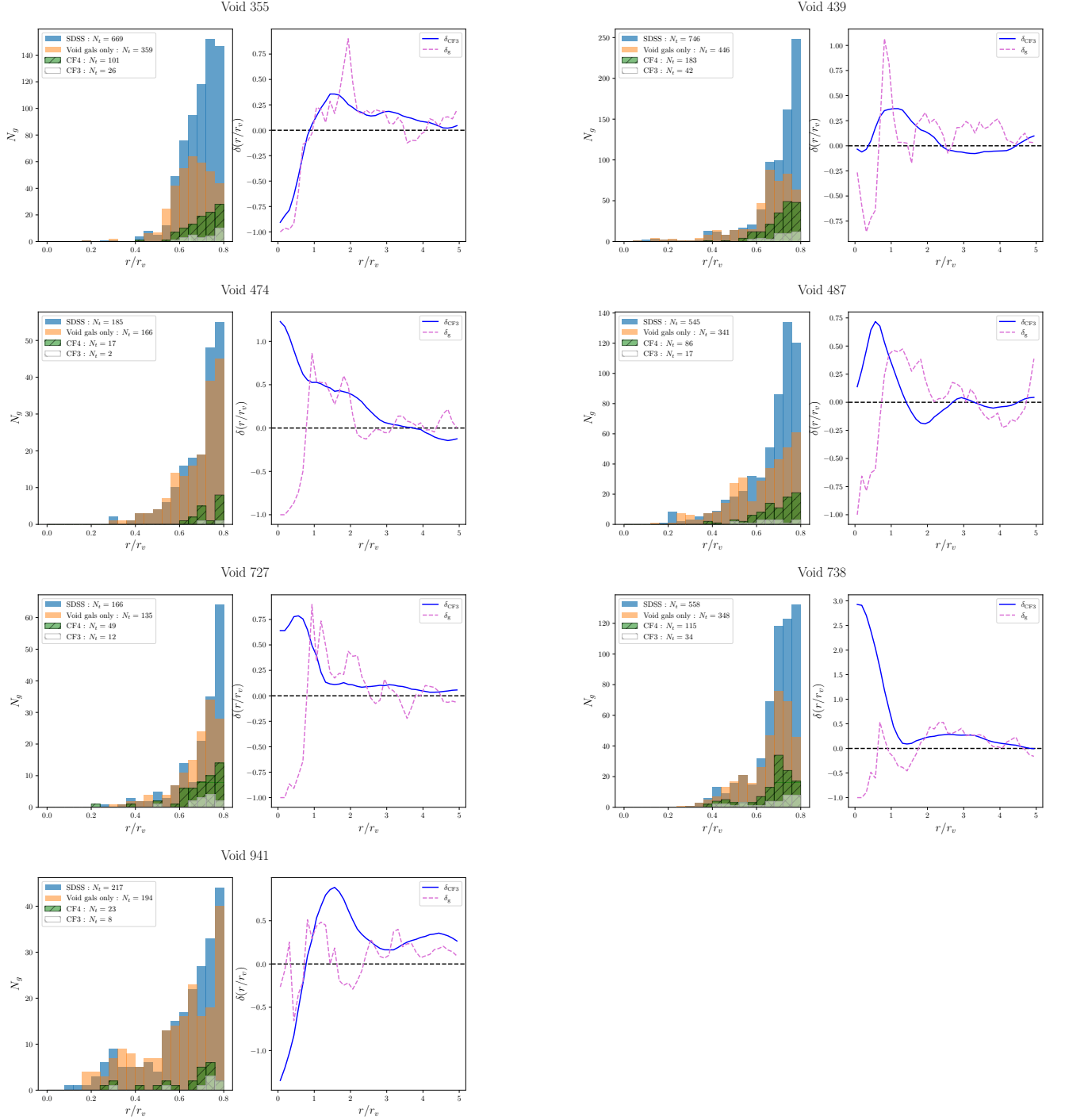


Fig. 5. Void radial density profiles. For each of the seven SDSS/CAVITY nearby voids that are included in CosmicFlows-3 volume we show on the left panel the radial number of galaxies and on the right panel the matter content computed from CF3 (blue) and from the galaxy number density in SDSS (pink). All seven voids are empty of galaxies near their center and roughly up to their effective radius. However four voids (474, 487, 727 and 738) display CF3 computed overdensities of matter in their center.

and importance of the *void-in-cloud* process in the buildup of the weblike matter distribution in the Universe. It also shows the importance of distinguishing these voids from the dominant fully expanding voids – the result of the *void-in-void* merging process – when we seek to study the role of voids in a cosmological setting (e.g. van de Weygaert 2016; Pisani et al. 2019) or when assessing their influence on galaxy formation and the galaxy star formation history (see Goldberg & Vogeley 2004; Lackner et al. 2012, for theoretical treatments).

The sample of 7 CAVITY voids is identified with a classical void finder from the SDSS redshift survey. It confirms that local voids are empty of galaxies near their center and roughly up to their effective radius. A different picture emerges when studying the velocity field in and around these voids. When assessing the dynamics of the void regions, and computing the matter content from the measured (CF3) velocity flows, in half of the cases, we would find that on the corresponding scale of the velocity flows these void regions would not be underdense. There are several

reasons why the mass and galaxy distribution around the sample voids may be different.

One factor is that of galaxy bias, with the galaxy population not entirely reflecting the underlying mass distribution. While we do not exclude this factor, we find that the strong levels of antibias that would be needed to explain our results are unrealistic (Peebles 2001; Gottlöber et al. 2003; Tinker et al. 2006; Ricciardelli et al. 2013; Bermejo et al. 2022). In fact, the overriding reason for the difference is to be found in the location of the voids with respect to their surroundings. Several sample voids are located in or to be identified with large underdensities in the mass distribution. The most interesting ones, slightly more than half of the sample, are found at the outer regions of the Coma-Leo and Virgo mass supercluster complexes.

A major part of the explanation for the difference between the galaxy distribution in and around these voids, and the inferred large scale mass distribution is the dynamical impact of the void environment. The void regions affiliated with large underdensities in the CF3 map of the Local Universe partake in the overall expansion of the region. The divergent velocity flow translates into a corresponding void mass density profile. It is a typical manifestation of the so-called *void-in-void* configuration that goes along with the hierarchical buildup of the void population (Sheth & van de Weygaert 2004).

However, in our void sample we find that the majority of CAVITY voids most likely appear to belong to the class of voids that are not expanding along three directions, and may even contract along 1 or 2 dimensions. These *void-in-cloud* voids (Sheth & van de Weygaert 2004) represent the majority of underdense regions in the mass distribution, and in the hierarchical buildup of structure are often found at the boundaries of large voids and surrounding overdense filaments and walls. The flow in and around these voids is largely dominated by the dynamical - tidal - influence of the nearby overdense filaments and walls. This translates into an anisotropic, in some cases even fully collapsing, flow field in and around the void, which explains the difference between the galaxy underdensity and the implied mass distribution, which includes the contribution from the surrounding overdense large scale structure. Hence, while on the large linear scales one finds the overdensity as it takes into account the large scale surroundings, on smaller scales one would recover the underdensity that is also seen in the galaxy distribution. It explains why the galaxy counts may hint at a local CAVITY, while the CF3 velocity flow would suggest otherwise.

Within the context of the hierarchically evolving void population, and the role of the surroundings in the evolution of voids, we may also find the merging of voids with overdense walls or filaments. A recent theoretical study (Vallés-Pérez et al. 2021) found that $\sim 10\%$ of the mass in voids at $z = 0$ may be accreted from overdense regions, and even reaching values beyond 35% for a fair fraction of voids.

While the present analysis of a limited void sample demonstrates the potential for studying voids in relation to their large scale environment, we expect exciting and statistically representative results on the Local Universe void population from the just released CosmicFlows-4 dataset of galaxy distances which includes the entire SDSS volume.

Acknowledgements. HC is grateful to the Institut Universitaire de France for its support. HC, MA, DG acknowledge support from the CNES. RvdW is grateful to Miguel Aragon-Calvo, Job Feldbrugge, Roi Kugul, Bernard Jones, Georg Wilding and Raul Bermejo on numerous discussions on the nature of voids and the role of topological bias. SDP is grateful to the Fonds de Recherche du Québec - Nature et Technologies and acknowledges financial support from the Spanish Ministerio de Economía y Competitividad under grant PID2019-

107408GB-C44, from Junta de Andalucía Excellence Project P18-FR-2664, and also acknowledge support from the State Agency for Research of the Spanish MCIU through the ‘Center of Excellence Severo Ochoa’ award for the Instituto de Astrofísica de Andalucía (SEV-2017-0709). E.F. is grateful to the Spanish ‘Ministerio de Ciencia e Innovación and from the European Regional Development Fund (FEDER) via grants PID2020-224414GB-I00 and PID2020-113689GB-I00, and from the ‘Junta de Andalucía’ (Spain) local government through the FQM108 and A-FQM-510-UGR20 projects. L.G. acknowledges financial support from the Spanish Ministerio de Ciencia e Innovación (MCIN), the Agencia Estatal de Investigación (AEI) 10.13039/501100011033, and the European Social Fund (ESF) ‘Investing in your future’ under the 2019 Ramón y Cajal program RYC2019-027683-I and the PID2020-115253GA-I00 HOST-FLOWS project, from Centro Superior de Investigaciones Científicas (CSIC) under the PIE project 20215AT016, and the program Unidad de Excelencia María de Maeztu CEX2020-001058-M. KK gratefully acknowledges funding from the German Research Foundation (DFG) in the form of an Emmy Noether Research Group (grant number KR4598/2-1, PI Kreckel). SP and VQ acknowledge support by the Spanish Ministerio de Ciencia e Innovación (MICINN, grant PID2019-107427GB-C33) and by the Generalitat Valenciana (grant PROMETEO/2019/071). JR acknowledges support from the State Research Agency (AEI-MCINN) of the Spanish Ministry of Science and Innovation under the grant ‘The structure and evolution of galaxies and their central regions’ with reference PID2019-105602GB-I00/10.13039/501100011033, funding granted for his Margarita Salas Fellowship by the Ministry of Universities granted by Order UNI/551/2021 of May 26, as well as funding by the European Union-Next Generation EU Funds. MSP acknowledges support from the Spanish Ministry of Science and Innovation through project AYA2017-88007-C3-2-P.

References

- Aragon-Calvo, M. A. & Szalay, A. S. 2013, MNRAS, 428, 3409
Aragon-Calvo, M. A., van de Weygaert, R., Araya-Melo, P. A., Platen, E., & Szalay, A. S. 2010, MNRAS, 404, L89
Bermejo, R., Wilding, G., van de Weygaert, R., et al. 2022, arXiv e-prints, arXiv:2206.14655
Bertschinger, E. 1985, ApJ, 295, 1
Beygu, B., Kreckel, K., van der Hulst, J. M., et al. 2016, MNRAS, 458, 394
Beygu, B., Peletier, R. F., van der Hulst, J. M., et al. 2017, MNRAS, 464, 666
Blumenthal, G. R., da Costa, L. N., Goldwirth, D. S., Lecar, M., & Piran, T. 1992, ApJ, 388, 234
Bond, J., Kofman, L., & Pogosyan, D. 1996, Nature, 380, 603
Borzyszkowski, M., Porciani, C., Romano-Díaz, E., & Galardi, E. 2017, MNRAS, 469, 594
Bos, E. G. P., van de Weygaert, R., Dolag, K., & Pettorino, V. 2012, MNRAS, 426, 440
Braun, E., Dekel, A., & Shapiro, P. R. 1988, ApJ, 328, 34
Cai, Y.-C., Padilla, N., & Li, B. 2015, MNRAS, 451, 1036
Cautun, M., Cai, Y.-C., & Frenk, C. S. 2016, MNRAS, 457, 2540
Cautun, M., van de Weygaert, R., Jones, B. J. T., & Frenk, C. S. 2014, MNRAS, 441, 2923
Courtis, H. M., Hoffman, Y., Tully, R. B., & Gottlöber, S. 2012, ApJ, 744, 43
Davis, M. & Peebles, P. J. E. 1983, ApJ, 267, 465
de Lapparent, V., Geller, M. J., & Huchra, J. P. 1986, ApJ, 302, L1
Domínguez-Gómez, J., Lisenfeld, U., Pérez, I., et al. 2022, A&A, 658, A124
Dubinski, J., da Costa, L. N., Goldwirth, D. S., Lecar, M., & Piran, T. 1993, ApJ, 410, 458
El-Ad, H. & Piran, T. 1997, ApJ, 491, 421
Ganeshaiah Veena, P., Cautun, M., Tempel, E., van de Weygaert, R., & Frenk, C. S. 2019, MNRAS, 487, 1607
Goh, T., Primack, J., Lee, C. T., et al. 2019, MNRAS, 483, 2101
Goldberg, D. M. & Vogeley, M. S. 2004, ApJ, 605, 1
Gottlöber, S., Łokas, E. L., Klypin, A., & Hoffman, Y. 2003, MNRAS, 344, 715
Graziani, R., Courtis, H. M., Lavaux, G., et al. 2019, MNRAS, 488, 5438
Hahn, O., Porciani, C., Carollo, C. M., & Dekel, A. 2007, MNRAS, 375, 489
Hamaus, N., Pisani, A., Sutter, P. M., et al. 2016, Phys. Rev. Lett., 117, 091302
Hamaus, N., Sutter, P. M., & Wandelt, B. D. 2014, Phys. Rev. Lett., 112, 251302
Hellwing, W. A., Cautun, M., van de Weygaert, R., & Jones, B. T. 2021, Phys. Rev. D, 103, 063517
Hoyle, F. & Vogeley, M. S. 2004, ApJ, 607, 751
Huchra, J. P., Macri, L. M., Masters, K. L., et al. 2012, ApJS, 199, 26
Icke, V. 1984, MNRAS, 206, 1P
Kirshner, R. P., Oemler, A., J., Schechter, P. L., & Smetman, S. A. 1981, ApJ, 248, L57
Kreckel, K., Platen, E., Aragón-Calvo, M. A., et al. 2012, AJ, 144, 16
Kreckel, K., Platen, E., Aragón-Calvo, M. A., et al. 2011, AJ, 141, 4
Lackner, C. N., Cen, R., Ostriker, J. P., & Joing, M. R. 2012, MNRAS, 425, 641
Lavaux, G. & Wandelt, B. D. 2010, MNRAS, 403, 1392

- Lavaux, G. & Wandelt, B. D. 2012, *ApJ*, 754, 109
- Pan, D. C., Vogeley, M. S., Hoyle, F., Choi, Y.-Y., & Park, C. 2012, *MNRAS*, 421, 926
- Paranjape, A., Hahn, O., & Sheth, R. K. 2018, *MNRAS*, 476, 3631
- Park, D. & Lee, J. 2007, *Phys. Rev. Lett.*, 98, 081301
- Paz, D., Lares, M., Ceccarelli, L., Padilla, N., & Lambas, D. G. 2013, *MNRAS*, 436, 3480
- Peebles, P. J. E. 1980, *The large-scale structure of the universe*
- Peebles, P. J. E. 2001, *ApJ*, 557, 495
- Pérez, I. & al. 2023, *MNRAS*
- Perico, E. L. D., Voivodic, R., Lima, M., & Mota, D. F. 2019, *A&A*, 632, A52
- Pisani, A., Massara, E., Spergel, D. N., et al. 2019, *BAAS*, 51, 40
- Pisani, A., Sutter, P. M., Hamaus, N., et al. 2015, *Phys. Rev. D*, 92, 083531
- Platen, E., van de Weygaert, R., & Jones, B. J. T. 2007, *MNRAS*, 380, 551
- Pomarède, D., Hoffman, Y., Courtois, H. M., & Tully, R. B. 2017, *ApJ*, 845, 55
- Ricciardelli, E., Quilis, V., & Planelles, S. 2013, *MNRAS*, 434, 1192
- Rojas, R. R., Vogeley, M. S., Hoyle, F., & Brinkmann, J. 2004, *ApJ*, 617, 50
- Rojas, R. R., Vogeley, M. S., Hoyle, F., & Brinkmann, J. 2005, *ApJ*, 624, 571
- Roth, M. M., Kelz, A., Fechner, T., et al. 2005, *PASP*, 117, 620
- Sheth, R. K. & van de Weygaert, R. 2004, *MNRAS*, 350, 517
- Tinker, J. L., Weinberg, D. H., & Warren, M. S. 2006, *ApJ*, 647, 737
- Tully, R. B., Courtois, H., Hoffman, Y., & Pomarède, D. 2014, *Nature*, 513, 71
- Tully, R. B., Courtois, H. M., & Sorce, J. G. 2016, *AJ*, 152, 50
- Tully, R. B., Kourkchi, E., Courtois, H. M., et al. 2022, *arXiv e-prints*, arXiv:2209.11238
- Vallés-Pérez, D., Quilis, V., & Planelles, S. 2021, *ApJ*, 920, L2
- van de Weygaert, R. 2016, in *The Zeldovich Universe: Genesis and Growth of the Cosmic Web*, ed. R. van de Weygaert, S. Shandarin, E. Saar, & J. Einasto, Vol. 308, 493–523
- van de Weygaert, R. & Babul, A. 1994, *ApJ*, 425, L59
- van de Weygaert, R. & Platen, E. 2011, in *International Journal of Modern Physics Conference Series*, Vol. 1, International Journal of Modern Physics Conference Series, 41–66
- van de Weygaert, R. & van Kampen, E. 1993, *MNRAS*, 263, 481
- Yan, H., Fan, Z., & White, S. D. M. 2013, *MNRAS*, 430, 3432

Appendix A: Void Density and Velocity Profiles

One may analytically compute the expected density and velocity profiles of isolated spherical voids, into the far nonlinear regime, up to the moment that voids experience shell crossing at their boundaries (for a review see van de Weygaert 2016). The explicit expression for the density and velocity profiles for an isolated spherical voids may be found in Sheth & van de Weygaert (2004).

One major result is that voids have a characteristic density and evolution time, that of shell crossing. For a spherical void this happens when it reaches a nonlinear density contrast $\delta \sim -0.8$ (ie. 20% of the global cosmic density), by which time the void has expanded by a factor ~ 1.7 . It corresponds to a linear density contrast $\delta_{lin} = -2.81$ (this is to be compared to the 1.69 for collapse of spherical overdensities).

A.1. Void Density Profiles

We may also use the expansion of isolated spherical voids to understand the overall density and velocity profiles of voids (see also van de Weygaert 2016) because they are underdense, they expand with respect to the background, and while interior shells expand faster than the outer ones. Due to the differential expansion of the interior mass shells, we get an accumulation of mass near the exterior and boundary of the void, meanwhile evening out the density distribution in the interior. It leads to a typical *bucket-shaped* density profile (opposite of tophat), with a linear "Hubble-like" void flow in the interior (your canonical voids is a "Hubble bubble"). For a wide range of initial radial profiles, voids will attain a bucket shaped profile.

Recently, there have been a range of studies on the issue of void density profiles, and the question whether they display universal behaviour (see e.g. Hamaus et al. 2014; Cautun et al. 2016). In a range of studies, (e.g Ricciardelli et al. 2013; Hamaus et al. 2014) concluded that spherically averaged density profiles of voids do indeed imply a universal density profile that could be characterized by 2 parameters.

Interestingly, these density profiles have a less prominent bucket shaped interior profile than those seen for the spherical voids. This may be understood from the fact that voids in general are not spherical, so that spherical averaging will lead to the mixing of different layers in the void's interior. The recent study by Cautun et al. (2016) confirms this: when taking into account the shape of voids, a remarkably strong bucket void density profile appears to surface.

A.2. Void Velocity Profiles

In the situation of a mature, evolved void, the velocity field of a void resembles that of a Hubble flow, in which the outflow velocity increases linearly with distance to the void center. In other words, voids are *super-Hubble bubbles* (Icke 1984). The linear velocity increase is a reflection of the corresponding density distribution: the near constant velocity divergence within the void conforms to the near uniform bucket-shaped interior density distribution that voids attain at more advanced stages.

It is straightforward to appreciate this from the *continuity equation*. For a uniform density field, it tells us that the velocity divergence in the void will be uniform, corresponding to a Hubble-like outflow. Because voids are emptier than the rest of the universe they will expand faster than the rest of the universe,

with a net velocity divergence equal to

$$\theta = \frac{\nabla \cdot \mathbf{v}}{H} = 3(\alpha - 1), \quad \alpha = H_{\text{void}}/H, \quad (\text{A.1})$$

where α is defined to be the ratio of the super-Hubble expansion rate of the void and the Hubble expansion of the universe. van de Weygaert & van Kampen (1993) confirmed that the velocity outflow field in viable cosmological scenarios does indeed resemble that of a superHubble expanding bubble. They established that the superHubble expansion rate is directly proportional to the nonlinear void density $\Delta(t)$,

$$H_{\text{void}}/H = -\frac{1}{3}f(\Omega)\Delta(t). \quad (\text{A.2})$$

This relation, known within the context of a linearly evolving spherical density perturbation, in the case of fully evolved voids appears to be valid on the basis of the *nonlinear* void density deficit. Several studies (e.g. Hamaus et al. 2014) have confirmed this finding for voids in a range of high resolution cosmological simulations.

The immediate implication is that voids should be considered as distinctly *nonlinear* objects.

A.3. Nonspherical Voids

One may wonder how far the nonsphericity of voids works out for their density and velocity profiles. Cautun et al. (2016) showed that this may severely influence the density and velocity profiles extracted of these voids and that spherical averaging may not always lead to a proper result. In the interpretation of the profiles presented in the draft, these effects will certainly play a role.

While the results above emanate from a rather unrealistic symmetric configuration - spherical, isolated - many studies have shown these to be rather representative for the major fully expanding voids in the galaxy distribution.

There is also a good reason why this is so: following the shellcrossing phase, the expansion of voids slows down (Bertschinger 1985). It was this realization, that prodded Dubinski et al. (1993) to point out that the large voids in redshift surveys are to be mostly identified with the voids that at the current epoch are undergoing shellcrossing.